THE JOURNAL OF PHYSICAL CHEMISTRY C
A JOURNAL OF THE AMERICAN CHEMICAL SOCIETY

pubs.acs.org/JPCC Article

Impact of Adsorption Configurations on Alcohol Dehydration over Alumina Catalysts

Rui Wang, Zhenchao Zhao,* Pan Gao, Kuizhi Chen, Zhehong Gan, Qiang Fu, and Guangjin Hou*

Cite This: *J. Phys. Chem. C* 2022, 126, 10073−10080 Read Online

ABSTRACT: The dehydration of alcohols to value-added chemicals using alumina catalysts has been industrialized decades ago; however, despite years of fundamental research, the molecular-level understanding of the reaction process is still lacking. Herein, the dehydration reactions of ethanol on two representative aluminas, *i.e.*, γ-Al_2O_3 and five-coordinated Al-rich Al_2O_3-nanosheet (Al_2O_3-NS), are comparatively investigated by a combination of solid-state NMR spectroscopy and reaction evaluations. NMR results reveal that the presence of hydroxyl groups nearby the Lewis acid sites (LASs) leads to different ethanol adsorption modes. The surface hydroxyls nearby LASs interfere with ethanol adsorption, which causes the methyl group to move away from the alumina surface and hinders the elimination of β-H, resulting in low reaction activity. In addition, the desorption property of surface hydroxyls will affect the dehydration reaction as they participate in the catalytic reaction cycles. Such effects may also explain the lower reaction activities for diethyl ether to ethylene compared with ethanol. Although both four- and five-coordinated Als are the possible active sites for ethanol dehydration, the reactivity of alcohol dehydration may also be substantially affected by the local environment of undercoordinated Als besides coordination numbers. These new insights demonstrate that the host−guest interaction regulated by the local environment of active sites plays an important role in the catalytic reaction.

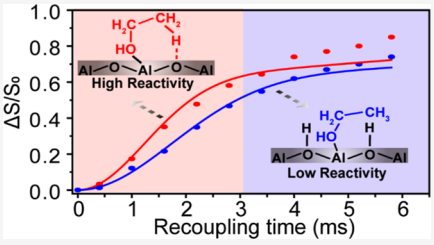

■ INTRODUCTION

Oxygenates such as alcohols derived from biomass are important renewable platform molecules for the chemical industry as alternatives to traditional petroleum resources.[1,2] Dehydration of oxygenates to olefins or ethers is an important transformation route to obtain high value-added fuel and chemical feedstocks by removing oxygen from oxygen-rich biomass.[3] Acid catalysts such as amorphous silica-alumina, zeolite, and alumina containing Brønsted acid sites (BASs), Lewis acid sites (LASs), or both can effectively catalyze the reaction.[4,5] Among these catalysts, γ-Al_2O_3 is practically used for alcohol dehydration reactions with high selectivity and stability.[6] Although γ-Al_2O_3 has been used as an alcohol dehydration catalyst for several decades,[7−9] the reaction mechanisms regarding critical reaction intermediates and active sites on the catalyst remain controversial.

Ethanol is one representative alcohol, and its monomolecular dehydration to ethylene and bimolecular dehydration to diethyl ether (DEE) are the typical transformation routes.[8] Besides, DEE will undergo a secondary reaction and be decomposed into ethylene and ethanol at a higher temperature.[10] Knöezinger et al. proposed that the active center was hydroxyl and basic center (surface oxygen atom), and olefins were derived from the E2-type elimination of alcohols based on a large number of studies on alcohol dehydration on γ-Al_2O_3.[11−14] In contrast, Roy et al. confirmed through Fourier transform infrared (FT-IR) spectra of pyridine adsorption that the acid sites on the surface of γ-Al_2O_3 were dominated by LASs,[15] and alcohols were first converted into alkoxy intermediates at the LASs and then followed by the removal of β-H to form olefins with the assistance of base sites.[16−19] Furthermore, Kwak et al. proposed that BAS was the active center for ethanol dehydration to ethylene on γ-Al_2O_3 calcined at a lower temperature (<473 K), while for high-temperature (>673 K) calcined γ-Al_2O_3, the ethanol adsorbed on the LASs would be converted into ethylene based on the ethanol temperature-programmed desorption (TPD) investigations.[20] Although the LASs have been increasingly proposed as the main active sites of ethanol dehydration in many theoretical calculation studies and kinetic models,[15,19,21,22] the detailed structure for the active site, specifically the coordination state of active Als, remains controversial. All of the surface three-, four-, and five-coordinated Als in the undercoordinated status are the probable active LASs for the dehydration reactions. Kwak et al. suggested that the five-coordinated Al was the active site for methanol dehydration.[20] In addition, both Hu[23] and Chen[24] have recently reported that the content of the five-coordinated Als was positively correlated with ethanol

Received: May 12, 2022
Revised: May 25, 2022
Published: June 9, 2022

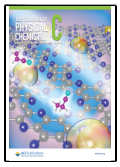

https://doi.org/10.1021/acs.jpcc.2c03303
J. Phys. Chem. C 2022, 126, 10073−10080

dehydration activity. However, Wischert et al. determined through theoretical calculations that the adsorption energy of N_2 on γ-Al_2O_3 increased with an increase in the coordination number of Al, indicating that Lewis acidity became stronger with the decrease of the coordination number of Al.[25] In addition to the coordination status of Als, trace additives such as Na^+ ions, the pressure of alcohol and water could also greatly affect the catalytic performance of alcohol dehydration.[15,19,26,27] Moreover, the low crystallinity of γ-Al_2O_3 caused by the inherent defects hinders the unambiguous determination of the structure of γ-Al_2O_3, which also makes it a great challenge to reveal its catalytically active sites.[28]

The solid-state nuclear magnetic resonance (NMR) technique is capable of extracting information about the chemical structure and local environment including the bonding/nonbonding spatial configuration at the atomic scale regardless of the crystalline/amorphous phases.[29] Various solid-state NMR techniques, including ^{27}Al and ^{17}O MQ MAS NMR, ^{1}H−^{1}H/^{17}O−^{17}O/^{27}Al−^{27}Al DQ MAS, and ^{1}H−^{27}Al HMQC NMR, have been employed to investigate the coordination states of Als, oxygen, and surface hydroxyl distribution of γ-Al_2O_3.[30−32] Thanks to NMR spectral editing techniques such as ^{1}H−^{27}Al HMQC[31] and ^{13}C−^{27}Al REAPDOR,[33] it is possible to reveal the direct interactions between reaction intermediates and active sites critical for the catalytic reactions. Herein, we conducted a comparative investigation on the dehydration reaction of ethanol on γ-Al_2O_3 and five-coordinated Al-rich Al_2O_3-nanosheet (Al_2O_3-NS) by solid-state NMR combined with TG-MS and reaction kinetic analysis. Al(V)-rich Al_2O_3-NS was chosen to signify the role of Al(V) because regular Al_2O_3 materials contain a very small quantity of Al(V) species. It was found that surface hydroxyl alters the adsorption configurations of ethanol on the surface of two aluminas, resulting in different reactivities. Moreover, the correlations between adsorbed ethanol/ethoxy and the active Als on the surface of alumina were clearly elucidated. It provided the first spectrometric evidence for the adsorption configuration of alcohol dominating the dehydration activities of catalysts.

■ METHODS

Synthesis of Al_2O_3-Nanosheet. Five-coordinated Al-rich Al_2O_3-nanosheet (Al_2O_3-NS) was synthesized following the previous report.[34] Typically, 6.46 g of $Al(NO_3)_3{\cdot}9H_2O$ (Sigma-Aldrich, 99.997% trace metals basis) and 9.21 g of urea (Aladdin, 99.999% metals basis) were dissolved in 60 mL of deionized water under magnetic stirring until a clear solution was obtained. The solution was transferred to a 100 mL Teflon-lined stainless autoclave and kept in a 100 °C oven for 48 h. Thereafter, the white precipitates were obtained by repeated washing with deionized water, centrifuged, and further dried at 110 °C for 12 h. Finally, it was calcined at 600 °C in a muffle furnace for 2 h with a ramp rate of 2 °C/min.

X-ray Powder Diffraction (XRD). X-ray powder diffraction (XRD) measurements were carried out on a Rigaku D/MAX-2500 X-ray diffractometer using Cu Kα radiation in the 2θ range of 10−80° at a scan rate of 5°/min.

TG-MS Measurements of Ethanol Desorption on Aluminas. The TG-MS experiments were performed on a Pyris Diamond TG/DTA (PerkinElmer) in a flow of N_2 (100 mL/min) at atmospheric pressure. About 10 mg of the sample was placed in an alumina crucible and heated from 20 to 800 °C with a ramp rate of 5 °C/min.

Solid-State NMR. Alumina samples were dehydrated at 350 or 550 °C for 16 and 5 h respectively, under a high vacuum of 10^{-4} Pa at a heating rate of 2 °C/min. After cooling to 25 °C, the dehydrated samples were immediately adsorbed with about 2 kPa of ^{13}C-labeled ethanol ($^{13}CH_3{}^{13}CH_2OH$), followed by vacuum desorption for 2 h, and transferred into a glovebox. For subsequent NMR experiments, the aluminas adsorbed with ethanol were treated at different temperatures under a vacuum of 0.1 kPa. All treated samples were packed into a sealed rotor in a glovebox for NMR testing to avoid exposure to air and moisture. The ^{13}C and ^{1}H NMR chemical shifts were referenced to adamantane (ADA), and the ^{27}Al NMR chemical shifts were referenced to 1 M $Al(NO_3)_3$ aqueous solution.

^{13}C CP/MAS NMR, ^{1}H detected 2D ^{1}H−^{13}C CP HETCOR (heteronuclear correlation),[35] and two-dimensional (2D) ^{13}C−^{13}C CP *J*-refocused INADEQUATE (incredible natural abundance double quantum transfer experiment)[36] MAS NMR experiments were carried out on a Bruker AVANCE NEO 800 spectrometer with resonance frequencies of 800.3 and 201.2 MHz for ^{1}H and ^{13}C, respectively, using a 3.2 mm HX probe at a spinning rate of 20 kHz. The Hartmann−Hahn condition for ^{1}H−^{13}C CP was optimized using adamantane (ADA), with a contact time of 2.5 ms and a recycle delay of 4 s. The ^{13}C MAS NMR spectra were acquired using a ^{13}C 90° pulse length of 3.3 μs with a 20 s recycle delay, where the ^{1}H SPINAL-64 decoupling was applied during the acquisition period. The ^{13}C detected 2D ^{1}H−^{13}C CP HETCOR spectrum was acquired on a Bruker AVANCE III HD 400 spectrometer with a 4.0 mm probe at a spinning rate of 12 kHz.

One-pulse ^{27}Al MAS NMR experiments were carried out on a Bruker AVANCE NEO 800 spectrometer with a 3.2 mm probe at a spinning rate of 20 kHz using a small flip angle of π/18 pulse of 0.5 μs. Ultrahigh-field (35.2 T) solid-state ^{1}H−^{27}Al HMQC NMR spectra were acquired using a series-connected hybrid (SCH) magnet at the National High Magnetic Field Laboratory (NHMFL) in Tallahassee, FL. A Bruker AVANCE NEO spectrometer was used with a 2.0 mm HXY MAS probe designed and constructed at the NHMFL and a sample spinning rate of 30 kHz. The dipolar recoupling SR4^{2}1 sequence was applied with a recoupling time of 0.4 ms, and 448 scans were accumulated. The ^{1}H detected and ^{27}Al detected ^{1}H−^{27}Al D-RINEPT NMR spectra were acquired at a Bruker AVANCE NEO 800 spectrometer using a 1.3 mm probe at a spinning rate of 60 kHz and a 3.2 mm probe at a spinning rate of 20 kHz, respectively. The recoupling time was set to 0.6 ms for the dipolar recoupling SR4^{2}1 sequence.

The ^{13}C−^{27}Al REAPDOR MAS NMR experiment (rotational-echo adiabatic-passage double-resonance)[37] was performed on the Bruker AVANCE III HD 400 spectrometer with a 4 mm probe using a frequency splitter REDOR-BOX at a spinning rate of 10 kHz. The CP contact time was 1500 μs, and a recycle delay of 4 s was used. Radio frequency field strengths were 62.5 kHz for ^{13}C and 63.8 kHz for ^{27}Al. The length of the adiabatic pulse applied on ^{27}Al was 33.33 us.

Reaction Evaluation. The catalytic reactions were performed on a quartz tube-packed fix-bed reactor (6 mm inner diameter). Alumina powders were pressed and sieved to get 40−60 mesh particle sizes. In a typical experiment, 0.01 g of catalyst (diluted by 0.09 g of quartz sand (40−60 mesh)) was activated at 350 °C for 16 h under nitrogen flow (20 mL/

https://doi.org/10.1021/acs.jpcc.2c03303
J. Phys. Chem. C 2022, 126, 10073−10080

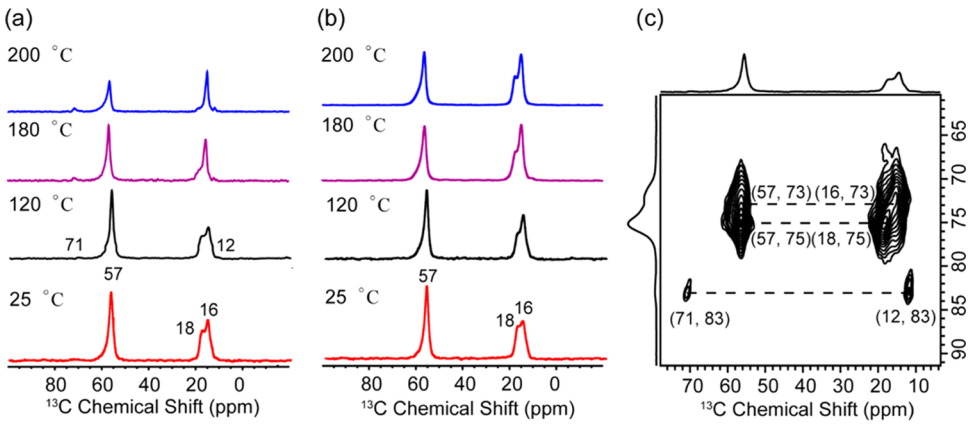

Figure 1. ^{13}C CP/MAS NMR spectra of ^{13}C-enriched ethanol adsorbed on dehydrated γ-Al_2O_3 (a) and Al_2O_3-NS (b) after desorption for 2 h at different temperatures. (c) ^{13}C−^{13}C *J*-based refocused INADEQUATE NMR spectrum of ethanol adsorption on dehydrated γ-Al_2O_3 and desorption at 120 °C for 2 h.

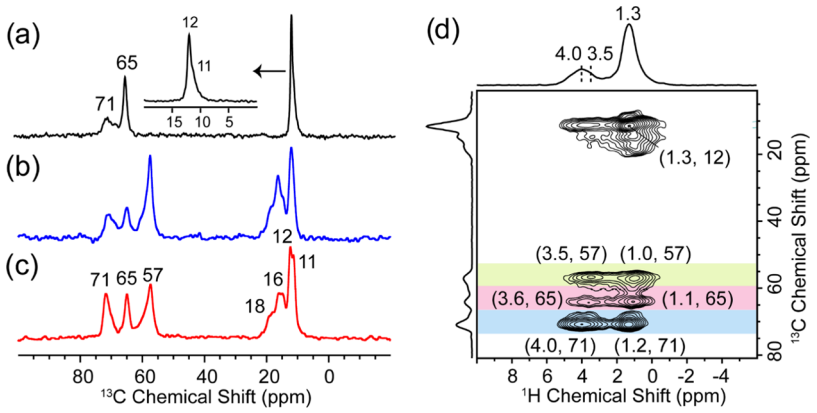

Figure 2. ^{13}C CP/MAS NMR spectra of (a) DEE adsorbed on dehydrated γ-Al_2O_3 and ^{13}C-DEE (containing ^{13}C-ethanol) adsorbed on Al_2O_3-NS (b) and γ-Al_2O_3 (c). (d) ^{1}H detected ^{13}C−^{1}H HETCOR NMR spectrum of ^{13}C-DEE (containing ^{13}C-ethanol) adsorbed on γ-Al_2O_3. The scan number is 12 288 for (a) and 128 for (b) and (c).

min) and cooled down to the temperature for the ethanol dehydration reaction. Ethanol was introduced by nitrogen (60 mL/min) from a bubbler with the temperature kept at 5 °C. The effluent products were quantitatively analyzed by an online gas chromatograph (Agilent 8890) with a PLOT-Q capillary column using an FID detector and He as the carrier gas.

■ RESULTS AND DISCUSSION

Basic Structural Properties of Aluminas. The XRD patterns and ^{27}Al MAS NMR spectra of the synthesized Al_2O_3-Nanosheet (Al_2O_3-NS) and γ-Al_2O_3 are shown in Figure S1. γ-Al_2O_3 shows broad characteristic peaks of the typical γ-phase of alumina, while Al_2O_3-NS is closer to the amorphous phase with minor peaks of γ-Al_2O_3. The ^{27}Al MAS NMR spectra (Figure S1b) show that there are more Al(V)s on Al_2O_3-NS (29%) than those of γ-Al_2O_3 (2%). ^{1}H−^{27}Al HMQC NMR spectra (Figure S2) can selectively extract the signals of surface Als by dipolar interactions between ^{27}Al and ^{1}H (hydroxyl groups) on the surface and also indicate that more Al(V)s present on the surface of Al_2O_3-NS. The Brunauer−Emmett−Teller (BET) surface areas from N_2 physisorption are 299 and 253 m^2/g for γ-Al_2O_3 and Al_2O_3-NS, respectively.

Ethanol Adsorption. The ^{13}C CP/MAS NMR spectra of ^{13}C-enriched ethanol ($^{13}CH_3{}^{13}CH_2OH$)-adsorbed samples after desorption at 25−200 °C and a representative 2D ^{13}C−^{13}C INADEQUATE NMR spectrum are shown in Figure 1. As shown in Figure 1a,b, the signals at 57 ppm and 16−18 ppm observed at 25 °C on both aluminas are assigned to methylene and methyl groups of ethanol, respectively. As the temperature was increased to 120 °C, two new weak signals at 71 and 12 ppm attributed to ethoxy were observed for γ-Al_2O_3,[38] which are generally identified as the intermediates for the formation of ethylene. The correlation peaks between methyl (16, 18 ppm) and methylene (57 ppm) groups for ethanol and methyl (12 ppm) and methylene (71 ppm) groups of ethoxy in ^{13}C−^{13}C *J*-based refocused INADEQUATE (Figure 1c) further confirm the above assignments. With the appearance of ethoxy, the peak intensity at 18 ppm is significantly weakened after 180−200 °C treatment, while that of Al_2O_3-NS does not change significantly, as shown in Figure 1b. It means that this kind of adsorbed ethanol (18 ppm) undergoes either desorption or consumption due to the higher reactivity. It should be noted that ethoxy on γ-Al_2O_3 is very sensitive to moisture, and only the signals of ethanol can be observed after exposure to air (Figure S3).[39] Unexpectedly, for Al_2O_3-NS with more Al(V)s that were considered as the active center in the ethanol dehydration reaction,[20] no signal of the ethoxy is observed in the entire temperature range up to 200 °C.

https://doi.org/10.1021/acs.jpcc.2c03303
J. Phys. Chem. C 2022, 126, 10073−10080

DEE Adsorption. The ^{13}C CP/MAS NMR spectrum (Figure 2a) of DEE adsorbed on γ-Al_2O_3 at 25 °C shows mainly four signals at 11, 12, 65, and 71 ppm. Interestingly, two evident signals of ethoxy at 71 and 12 ppm are observed, while the signals of ethanol are not observed, which highly suggests that DEE can be dissociatively adsorbed at Lewis acid (Al) and base (O) centers on γ-Al_2O_3 as two ethoxy groups even at 25 °C. Two new signals completely different from ethanol at 65 and 11 ppm can be assigned to the signal of DEE adsorbed on γ-Al_2O_3. It is also worth noting that the relative signal intensities of ethoxy generated by the dissociation of DEE on γ-Al_2O_3 are much stronger than those from the ethanol-adsorbed catalyst because the dissociation of DEE will not generate water. To further confirm these assignments, ^{13}C-DEE with residual ^{13}C-ethanol derived from ^{13}C-ethanol dehydration was adsorbed on the dehydrated γ-Al_2O_3 and Al_2O_3-NS, and the corresponding ^{13}C CP/MAS NMR spectra are shown in Figure 2b,c. All of the signals assigned to adsorbed ethanol, DEE, and ethoxy can be clearly observed. ^{1}H detected 2D $^{13}C-^{1}H$ HETCOR experiments with enhanced ^{1}H resolution combined with ^{1}H MAS NMR spectra and ^{13}C detected $^{13}C-^{1}H$ HETCOR NMR spectra (Figures S4 and S5) were performed to make a clear assignment of the signals of ^{1}H and correlated ^{13}C, as shown in Figure 2d, and the detailed signal assignments are listed in Table 1.

Table 1. Assignments of NMR Signals of Ethanol and Its Derivatives Adsorbed on γ-Al_2O_3

	^{1}H signal (ppm)		^{13}C signal (ppm)	
species	$-CH_2-$	$-CH_3$	$-CH_2-$	$-CH_3$
ethoxy	4.0	1.2	71	12
ethanol	3.5	1.0	57	16 and 18
DEE	3.6	1.1	65	11

Adsorption Modes of Ethanol. For both ethanol-adsorbed aluminas, two different signals of the methyl groups with different reactivities were observed, which may be caused by the different adsorption configurations of ethanol. $^{13}C-^{27}Al$ REAPDOR NMR experiments were carried out to study the spatial interaction between the ^{13}C atom of the methyl group and the ^{27}Al atom on the surface of γ-Al_2O_3. Figure 3 shows the representative one-dimensional (1D) $^{13}C-^{27}Al$ REAPDOR NMR spectra and the obtained dephasing curves of ethanol adsorbed on γ-Al_2O_3 at 25 °C. As in shown in Figure 3a, the intensity of the signal at 18 ppm decreases more significantly than 16 ppm, implying that there is closer spatial proximity and stronger dipolar interaction between the carbon atom of the methyl groups (18 ppm) and the surface Al atoms. Furthermore, the dephasing curve (Figure 3b) recording the signal attenuation value $\Delta S/S_0$ as a function of the recoupling time was fitted to obtain the internuclear distances, and the spatial distances between two kinds of ^{13}C (18 and 16 ppm) atoms and ^{27}Al atoms were quantitatively estimated, which are 3.44 and 3.86 Å, respectively. Considering that the adsorption sites on the surface of alumina should be LASs and hydroxyl groups, the observation of two different adsorption configurations of ethanol suggests that one may be absorbed on LAS and the other at hydroxyl; alternatively, ethanol is absorbed on LASs with different microenvironments. As these signals can be preserved even after 200 °C desorption for Al_2O_3-NS (Figure 1b), the strongly adsorbed ethanol with methyl signals at 18 and 16 ppm should result from LASs with different microenvironments, where methyl groups have different distances from the surface. For 550 °C dehydrated Al_2O_3-NS, as most hydroxyl groups were removed, the relative amount of adsorbed ethanol at 16 ppm decreased (Figure S6), implying that the signal at 16 ppm may be affected by the hydroxyl groups near LASs. The possible adsorption models are shown in Figure 3c−e. Since the methyl group has different distances from the surface of alumina, we infer that the signal at 16 ppm may be from the ethanol adsorption perturbed by hydroxyl groups near the LASs (Figure 3d,e) but different from adsorbed ethanol at 18 ppm (Figure 3c). The hydroxyl groups near the LASs make the adsorbed ethanol molecules more vertical to the surface as a steric hindrance, leading to a relatively longer average distance between methyl groups and the surface of catalysts.

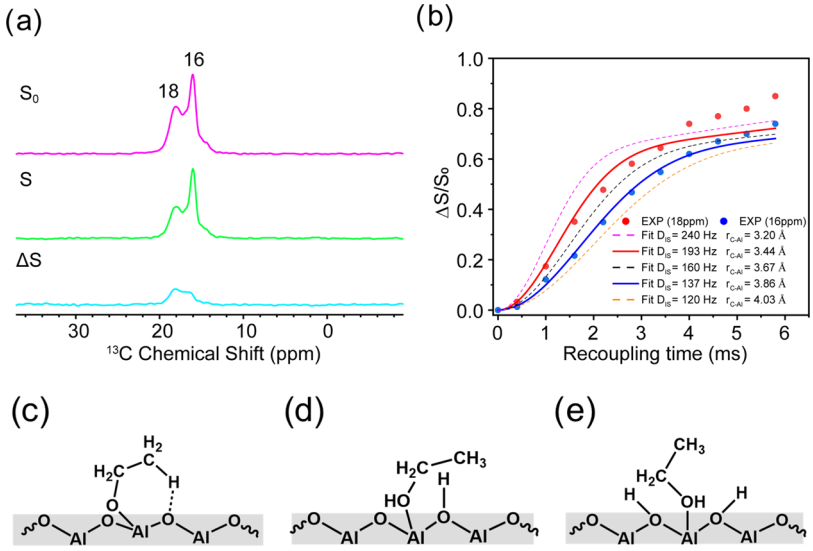

Figure 3. (a) 1D $^{13}C-^{27}Al$ REAPDOR NMR spectra of ^{13}C-ethanol adsorbed on γ-Al_2O_3 at 25 °C with a recoupling time of 1.6 ms. (b) $^{13}C-^{27}Al$ REAPDOR NMR spectra fitting curves of signals at 18 and 16 ppm. The proposed adsorption modes of ethanol on γ-Al_2O_3 are shown in (c) (18 ppm) and (d, e) (16 ppm).

https://doi.org/10.1021/acs.jpcc.2c03303
J. Phys. Chem. C 2022, 126, 10073−10080

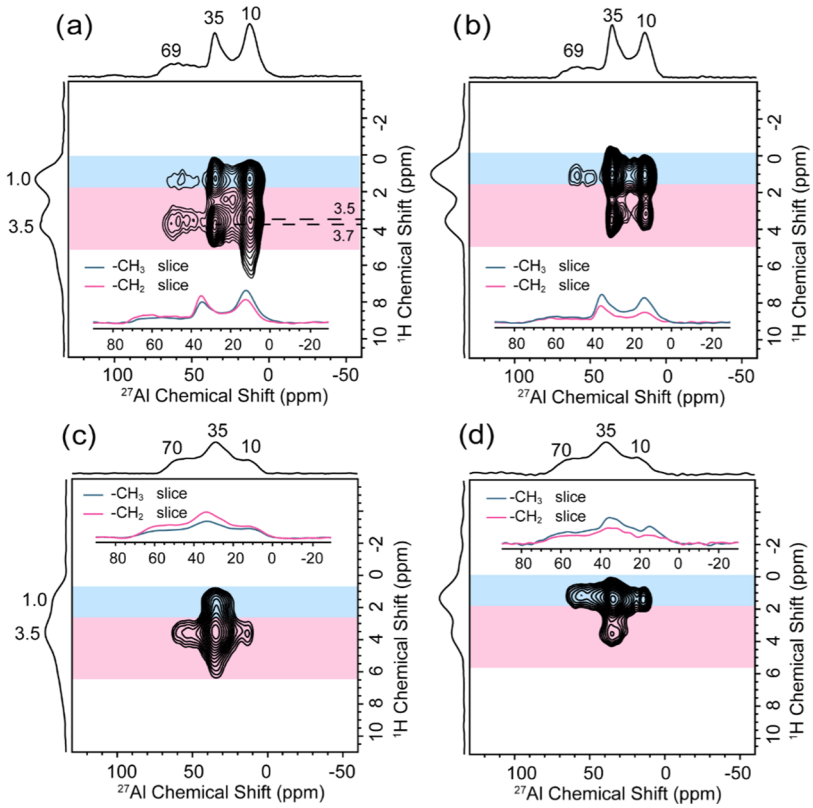

Figure 4. $^{1}H-^{27}Al$ D-RINEPT NMR spectra and slices from selected correlations of ^{13}C-ethanol adsorption on dehydrated catalysts. (a) γ-Al_2O_3 dehydrated at 350 °C, (b) γ-Al_2O_3 dehydrated at 550 °C, (c) Al_2O_3-NS dehydrated at 350 °C, (d) Al_2O_3-NS dehydrated at 550 °C.

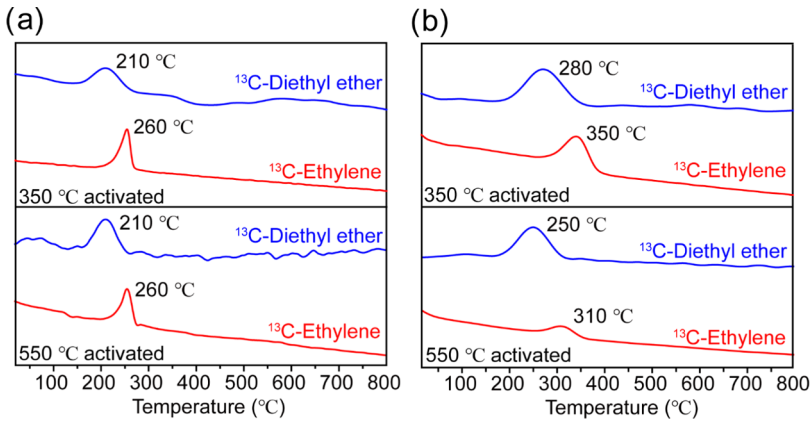

Figure 5. TG-MS analysis of ^{13}C-ethanol desorption on γ-Al_2O_3 (a) and Al_2O_3-NS (b) activated at 350 and 550 °C.

To clarify the configurations of different adsorption modes of ethanol molecules on alumina catalysts, $^{1}H-^{27}Al$ D-RINEPT NMR experiments were further conducted, and the spectra are shown in Figure 4. For γ-Al_2O_3, both the protons of methylene (3.5 ppm) and methyl (1.0 ppm) have strong correlation peaks with Al(V)s (35 ppm) and Al(VI)s (10 ppm). It is worth noting the protons of methylene groups of ethanol adsorbed at Al(V)s shift to a lower field at 3.7 ppm compared with those of ethanol (3.5 ppm) adsorbed at Al(VI)s. It is reasonable that Al(V)s and Al(VI)s are derived from Al(IV)s and Al(V)s, respectively, while Al(IV)s have stronger Lewis acidity than Al(V)s. Moreover, the $^{1}H-^{27}Al$ D-RINEPT NMR spectrum (Figure S7) of ^{13}C-DEE-adsorbed γ-Al_2O_3 demonstrates methylene groups of ethoxy also correlate with both Al(V)s and Al(VI)s. These results indicate both Al(IV) and Al(V) LASs on γ-Al_2O_3 are active adsorption sites. As is clearly shown in Figure 4a,b, the correlation signals between CH_3 and surface Als are stronger than those of CH_2, especially for the catalyst pre-dehydrated at 550 °C (Figure 4b), although theoretically CH_2 is closer to the surface than CH_3. It can be only explained that CH_3 is also very close to the surface of γ-Al_2O_3 and CH_3 groups have more H than CH_2 groups. In contrast, as for Al_2O_3-NS, the protons of ethanol are mainly correlated with Al(V)s. Moreover, the correlations between CH_2 groups of ethanol and surface Als for Al_2O_3-NS dehydrated at 350 °C are much stronger than those of CH_3 (Figure 4c). After the removal of most surface hydroxyl groups at 550 °C (Figure 4d), the correlation signals between CH_3 and surface Als become stronger than those of CH_2, similar to γ-Al_2O_3. All these results indicate that the surface hydroxyls

https://doi.org/10.1021/acs.jpcc.2c03303
J. Phys. Chem. C 2022, 126, 10073−10080

have a significant impact on the ethanol adsorption on alumina catalysts.

Reaction Evaluations. To study reaction behaviors of ethanol adsorbed on the catalysts, temperature-programmed surface reaction (TPSR) utilizing TG-MS was also carried out. As shown in Figure 5, DEE is first formed with the peak temperature at 210 °C and then ethylene is formed with the peak temperature at 260 °C for γ-Al_2O_3 activated (dehydrated) at 350 °C (Figure 5a), and no obvious change in the desorption peaks is observed for γ-Al_2O_3 activated at 550 °C. Whereas, the desorption peaks of DEE and ethylene at Al_2O_3-NS activated at 350 °C shift to higher temperatures at 280 and 350 °C, respectively (Figure 5b). When the activation temperature was elevated to 550 °C, desorption peaks of DEE and ethylene shifted to lower temperatures at 250 and 310 °C, respectively. The results indicated that ethanol adsorbed on γ-Al_2O_3 has higher reactivity to DEE and ethylene than Al(V)-rich Al_2O_3-NS. It is worth noting that the changes in desorption peaks of DEE and ethylene on Al_2O_3-NS imply that the active centers of Al_2O_3-NS are altered after high-temperature activation but not for γ-Al_2O_3.

The reaction performances of the alumina catalysts were further evaluated by a fixed-bed reactor. As shown in Figure S8a,b, DEE begins to be generated at a lower temperature on γ-Al_2O_3 (140 °C) than that on Al_2O_3-NS (170 °C). The formation of ethylene follows the same tendency on γ-Al_2O_3 (200 °C) and Al_2O_3-NS (240 °C). For γ-Al_2O_3, the formation of DEE and ethylene at a lower temperature is consistent with NMR and TPSR results. In addition, ethoxy is produced at a lower temperature (120 °C, Figure 1) than DEE, implying that DEE may originate from ethoxy. The reaction behavior of DEE over alumina catalysts was also studied, as shown in Figure S8c,d. At lower reaction temperatures, except for minor unknown impurity and ethanol in the DEE, there is no evolution of the products such as ethylene and ethanol. As the temperature increases, ethylene begins to be produced at temperatures above 260 and 280 °C for γ-Al_2O_3 and Al_2O_3-NS, respectively, accompanied by the appearance of ethanol. It indicates that the decomposition of DEE produces ethanol and ethylene at the same time. It is worth noting that the reaction activity of DEE to ethylene is significantly lower than that of ethanol on both alumina catalysts. The apparent activation energies (Figure S9) for the production of DEE from ethanol are 93 and 97 kJ/mol, while those of ethylene are 179 and 156 kJ/mol for γ-Al_2O_3 and Al_2O_3-NS, respectively. Although two catalysts exhibit similar activation energies for DEE formation, those for ethylene formation are significantly different.

Reaction Mechanism. Alcohol dehydration to olefins over alumina catalysts is generally recognized to proceed via an E2-type dehydration mechanism involving concerted cleavage of C_β−H over a base site and C−OH bond over an acid site. Our multinuclear and multidimensional NMR results demonstrate that ethanol molecules have two different adsorption configurations on the surface of alumina, and they possess different reactivities. It is found that ethanol and ethoxy can be adsorbed on Al(V)s and Al(VI)s, which means that both Al(IV)s and Al(V)s on the surface of alumina are the possible active sites for the ethanol dehydration reaction. In contrast, the local environments of these active sites determine their activities besides the coordination number of Als. For instance, Al(IV)s are not necessary more reactive than Al(V)s. Although most of the ethanol molecules are adsorbed on the Al(V)s for Al_2O_3-NS from ^{1}H−^{27}Al D-RINEPT NMR, their reactivities are lower than those adsorbed at γ-Al_2O_3. We noticed that Al(V)s were recently reported to populate on the surfaces and promote BAS formation in Al(V)-rich amorphous silica-aluminas (ASAs).[40] To exclude the impact of BASs, trimethylphosphine (TMP) adsorption capable of discriminating BASs and LASs was carried out for both γ-Al_2O_3 and Al_2O_3-NS, and ^{31}P MAS NMR spectra (Figure S10) show only signals near −50 ppm attributed to TMP adsorbed at LASs for both samples.[41] As previously reported, for ethanol dehydration to ethylene, a β-H elimination in the E2 dehydration mechanism plays important roles.[18,42] β-H elimination is strongly affected by the configuration of methyl groups and base properties of surface oxygen/hydroxyl species. In the reaction of DEE to ethylene, although ethoxy is formed at 25 °C, the formation of ethylene only occurs at a temperature near 300 °C significantly higher than ethanol, which means that the β-H elimination step may be more difficult. Ethanol adsorption can be perturbed by the surface hydroxyl groups, leading to different adsorption configurations as well as reactivities of ethanol on the alumina surface (Scheme 1a,b).

Scheme 1. Proposed Pathways for Ethanol Dehydration on γ-Al_2O_3: (a) Ethanol Adsorbed on Lewis Acid Sites Interfered by Hydroxyl Groups and (b) Ethanol Adsorbed on Lewis Acid Sites without Neighboring Hydroxyl Groups[a]

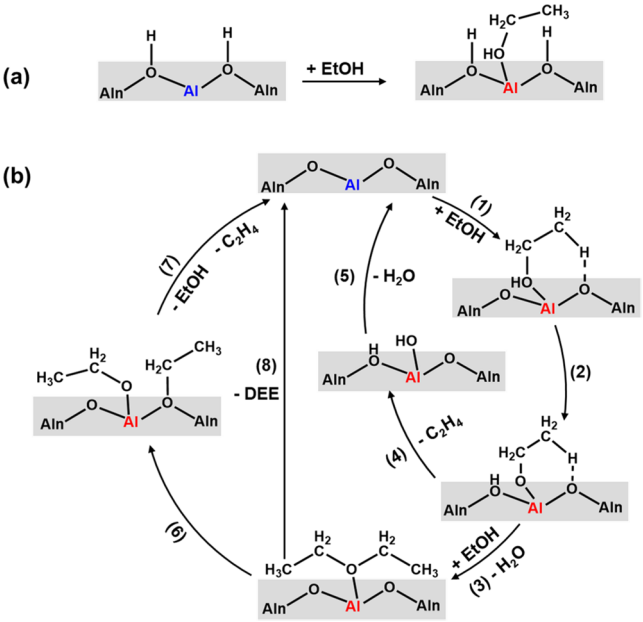

[a]Al atom marked in blue represents Al(IV) or Al(V), while Al atoms marked in red correspond to Al(V) and Al(VI).

Since the hydroxyl groups of both aluminas mainly exist in the form of bridged hydroxyl groups,[43] ethanol adsorption as Al(IV) or Al(V) without neighboring hydroxyl groups may have much higher reactivities to form ethoxy and DEE (Scheme 1b, step 1−3). Ethoxy groups will proceed with β-H elimination to form ethylene, and then the surface hydroxyl groups will dehydrated to complete the catalytic cycles (steps 4 and 5). It should be noted here that dehydration of surface hydroxyl groups should also impact the apparent activation energy for the dehydration reaction. Although the dehydration temperature of ethanol to ethylene is lower for γ-Al_2O_3, the apparent activation energy from the fixed-bed reaction is higher than Al_2O_3-NS, as the hydroxyl groups on Al_2O_3-NS are

https://doi.org/10.1021/acs.jpcc.2c03303
J. Phys. Chem. C 2022, 126, 10073−10080

more readily desorbed.[43] When DEE is further dehydrated to ethylene, the two adjacent ethoxys from DEE dissociative adsorption may also hinder the β-H elimination on the surface of alumina, and therefore, ethylene and ethanol were produced simultaneously with lower activity (steps 6 and 7).

■ CONCLUSIONS

A comparative study on the dehydration reaction mechanism of ethanol on commercial γ-Al_2O_3 and Al(V)-rich Al_2O_3-NS was carried out by a combination of NMR techniques, TG-MS, and reaction kinetic analysis. Two different adsorption configurations of ethanol on LASs were observed. Ethanol adsorption is perturbed by nearby surface hydroxyl groups, which causes the methyl groups to move away from the surface of alumina, thus hindering the β-H elimination and leading to lower reactivity for ethylene production. It is also found that both Al(IV)s and Al(V)s as the LASs contribute to the catalytic dehydration of ethanol. The formation and desorption of surface hydroxyls are indispensable to complete the catalytic reaction cycle, and hydroxyl groups will also impact the reactivities. These effects may also be applicable for DEE to the ethylene reaction, showing lower activity than ethanol. The catalytic performance of commercial γ-Al_2O_3 for ethanol dehydration is significantly superior to that of Al(V)-rich Al_2O_3-NS, although Al(V) was proposed as the active center, revealing that the reactivity of ethanol dehydration is also significantly affected by the local environment of under-coordinated Als.

■ ASSOCIATED CONTENT

Supporting Information

The Supporting Information is available free of charge at https://pubs.acs.org/doi/10.1021/acs.jpcc.2c03303.

Figures of XRD patterns; ^{27}Al MAS NMR; 1D ^{1}H−^{27}Al HMQC NMR spectra; ^{13}C CP/MAS NMR spectra; ^{1}H MAS NMR spectra; ^{13}C detected ^{13}C−^{1}H HETCOR NMR spectra; ^{1}H−^{27}Al D-RINEPT NMR spectra and ^{13}C MAS NMR spectra; GC signals for ethanol dehydration; and fitted plots of the apparent activation energy (PDF)

■ AUTHOR INFORMATION

Corresponding Authors

Zhenchao Zhao − *Key Laboratory of the Ministry of Education for Advanced Catalysis Materials, Institute of Physical Chemistry, Zhejiang Normal University, Jinhua 321004, China; State Key Laboratory of Catalysis, Dalian Institute of Chemical Physics, Chinese Academy of Sciences, Dalian 116023, China;* orcid.org/0000-0002-3715-4308; Email: zhaoenc@dicp.ac.cn

Guangjin Hou − *State Key Laboratory of Catalysis, Dalian Institute of Chemical Physics, Chinese Academy of Sciences, Dalian 116023, China;* orcid.org/0000-0001-8216-863X; Email: ghou@dicp.ac.cn

Authors

Rui Wang − *Zhang Dayu School of Chemistry, Dalian University of Technology, Dalian, Liaoning 116024, China; State Key Laboratory of Catalysis, Dalian Institute of Chemical Physics, Chinese Academy of Sciences, Dalian 116023, China*

Pan Gao − *State Key Laboratory of Catalysis, Dalian Institute of Chemical Physics, Chinese Academy of Sciences, Dalian 116023, China;* orcid.org/0000-0003-4997-6218

Kuizhi Chen − *State Key Laboratory of Catalysis, Dalian Institute of Chemical Physics, Chinese Academy of Sciences, Dalian 116023, China; National High Magnetic Field Laboratory, Tallahassee, Florida 32310, United States;* orcid.org/0000-0002-9853-7070

Zhehong Gan − *National High Magnetic Field Laboratory, Tallahassee, Florida 32310, United States;* orcid.org/0000-0002-9855-5113

Qiang Fu − *Zhang Dayu School of Chemistry, Dalian University of Technology, Dalian, Liaoning 116024, China; State Key Laboratory of Catalysis, Dalian Institute of Chemical Physics, Chinese Academy of Sciences, Dalian 116023, China;* orcid.org/0000-0001-5316-6758

Complete contact information is available at: https://pubs.acs.org/10.1021/acs.jpcc.2c03303

Notes

The authors declare no competing financial interest.

■ ACKNOWLEDGMENTS

The authors are grateful for the financial support from the National Natural Science Foundation of China (nos. 21972143, 22002165, 21773230, 91945302, 21603022, and 21773233), Liao Ning Revitalization Talents Program (XLYC1807207), Dalian Youth Science and Technology Star Program (2019RQ079), DICP&QIBEBT UN201808, and DICP I202104. A portion of this work was performed at the National High Magnetic Field Laboratory, which is supported by the National Science Foundation Cooperative Agreement No. DMR-1644779 and the State of Florida. Development of the SCH magnet and NMR instrumentation was supported by NSF (DMR-1039938 and DMR-0603042) and NIH P41 GM122698.

■ REFERENCES

(1) Stöcker, M. Biofuels and Biomass-to-Liquid Fuels in the Biorefinery: Catalytic Conversion of Lignocellulosic Biomass Using Porous Materials. *Angew. Chem., Int. Ed.* **2008**, *47*, 9200−9211.

(2) Alonso, D. M.; Bond, J. Q.; Dumesic, J. A. Catalytic Conversion of Biomass to Biofuels. *Green Chem.* **2010**, *12*, 1493−1513.

(3) Guo, N.; Caratzoulas, S.; Doren, D. J.; Sandler, S. I.; Vlachos, D. G. A Perspective on the Modeling of Biomass Processing. *Energy Environ. Sci.* **2012**, *5*, 6703−6716.

(4) Wang, Z.; O'Dell, L. A.; Zeng, X.; Liu, C.; Zhao, S.; Zhang, W.; Gaborieau, M.; Jiang, Y.; Huang, J. Insight into Three-Coordinate Aluminum Species on Ethanol-to-Olefin Conversion over ZSM-5 Zeolites. *Angew. Chem., Int. Ed.* **2019**, *58*, 18061−18068.

(5) Zhou, X.; Wang, C.; Chu, Y.; Xu, J.; Wang, Q.; Qi, G.; Zhao, X.; Feng, N.; Deng, F. Observation of An Oxonium Ion Intermediate in Ethanol Dehydration to Ethene on Zeolite. *Nat. Commun.* **2019**, *10*, No. 1961.

(6) Prins, R. On the Structure of γ-Al_2O_3. *J. Catal.* **2020**, *392*, 336−346.

(7) Adkins, H.; Perkins, P. P. Dehydration of Alcohols over Alumina. *J. Am. Chem. Soc.* **1925**, *47*, 1163−1167.

(8) Knözinger, H.; Köhne, R. The Dehydration of Alcohols over Alumina: I. The Reaction Scheme. *J. Catal.* **1966**, *5*, 264−270.

(9) Lane, R.; Lane, B.; Phillips, C. The Use of Stopped-flow Gas Chromatography to Study the Catalytic Dehydration of Alcohols. *J. Catal.* **1970**, *18*, 281−296.

(10) DeWilde, J. F.; Bhan, A. Kinetics and Site Requirements of Ether Disproportionation on γ-Al_2O_3. *Appl. Catal., A* **2015**, *502*, 361−369.
(11) Knözinger, H.; Bühl, H.; Ress, E. The Dehydration of Alcohols over Alumina: VII. The Dependence of Reaction Direction on the Substrate Structure. *J. Catal.* **1968**, *12*, 121−128.
(12) Knözinger, H.; Bühl, H.; Kochloefl, K. The Dehydration of Alcohols on Alumina: XIV. Reactivity and Mechanism. *J. Catal.* **1972**, *24*, 57−68.
(13) Knoezinger, H.; Scheglila, A.; Watson, A. M. Dehydration of Alcohols over Alumina. VIII. Ether Formation from the Deuterated Methanols CH_3OH, CD_3OH, CH_3OD, and CD_3OD. *J. Phys. Chem. A* **1968**, *72*, 2770−2774.
(14) Knözinger, H.; Scheglila, A. The Dehydration of Alcohols on Alumina: XII. Kinetic Isotope Effects in the Olefin Formation from Butanols. *J. Catal.* **1970**, *17*, 252−263.
(15) Roy, S.; Mpourmpakis, G.; Hong, D.-Y.; Vlachos, D. G.; Bhan, A.; Gorte, R. J. Mechanistic Study of Alcohol Dehydration on γ-Al_2O_3. *ACS Catal.* **2012**, *2*, 1846−1853.
(16) Srinivasan, P. D.; Khivantsev, K.; Tengco, J. M. M.; Zhu, H.; Bravo-Suárez, J. J. Enhanced Ethanol Dehydration on γ-Al_2O_3 Supported Cobalt Catalyst. *J. Catal.* **2019**, *373*, 276−296.
(17) Phung, T. K.; Lagazzo, A.; Rivero Crespo, M. Á.; Sánchez Escribano, V.; Busca, G. A Study of Commercial Transition Aluminas and of Their Catalytic Activity in the Dehydration of Ethanol. *J. Catal.* **2014**, *311*, 102−113.
(18) DeWilde, J. F.; Chiang, H.; Hickman, D. A.; Ho, C. R.; Bhan, A. Kinetics and Mechanism of Ethanol Dehydration on γ-Al_2O_3: The Critical Role of Dimer Inhibition. *ACS Catal.* **2013**, *3*, 798−807.
(19) Larmier, K.; Chizallet, C.; Cadran, N.; Maury, S.; Abboud, J.; Lamic-Humblot, A.-F.; Marceau, E.; Lauron-Pernot, H. Mechanistic Investigation of Isopropanol Conversion on Alumina Catalysts: Location of Active Sites for Alkene/Ether Production. *ACS Catal.* **2015**, *5*, 4423−4437.
(20) Kwak, J. H.; Mei, D.; Peden, C. H. F.; Rousseau, R.; Szanyi, J. (100) Facets of γ-Al_2O_3: The Active Surfaces for Alcohol Dehydration Reactions. *Catal. Lett.* **2011**, *141*, 649−655.
(21) Christiansen, M. A.; Mpourmpakis, G.; Vlachos, D. G. Density Functional Theory-Computed Mechanisms of Ethylene and Diethyl Ether Formation from Ethanol on γ-Al_2O_3(100). *ACS Catal.* **2013**, *3*, 1965−1975.
(22) Jenness, G. R.; Christiansen, M. A.; Caratzoulas, S.; Vlachos, D. G.; Gorte, R. J. Site-Dependent Lewis Acidity of γ-Al_2O_3 and Its Impact on Ethanol Dehydration and Etherification. *J. Phys. Chem. C* **2014**, *118*, 12899−12907.
(23) Hu, J. Z.; Xu, S.; Kwak, J. H.; Hu, M. Y.; Wan, C.; Zhao, Z.; Szanyi, J.; Bao, X.; Han, X.; Wang, Y.; Peden, C. H. High Field ^{27}Al MAS NMR and TPD Studies of Active Sites in Ethanol Dehydration Using Thermally Treated Transitional Aluminas as Catalysts. *J. Catal.* **2016**, *336*, 85−93.
(24) Chen, S.; Chen, J.; Qu, T.; Xiang, K.; Zhang, Y.; Hao, P.; Peng, L.; Xie, M.; Guo, X.; Ding, W. Crown Ether Induced Assembly to γ-Al_2O_3 Nanosheets with Rich Pentacoordinate Al^{3+} Sites and High Ethanol Dehydration Activity. *Appl. Surf. Sci.* **2018**, *457*, 626−632.
(25) Wischert, R.; Laurent, P.; Coperet, C.; Delbecq, F.; Sautet, P. Gamma-Alumina: the Essential and Unexpected Role of Water for the Structure, Stability, and Reactivity of "Defect" Sites. *J. Am. Chem. Soc.* **2012**, *134*, 14430−14449.
(26) DeWilde, J. F.; Czopinski, C. J.; Bhan, A. Ethanol Dehydration and Dehydrogenation on γ-Al_2O_3: Mechanism of Acetaldehyde Formation. *ACS Catal.* **2014**, *4*, 4425−4433.
(27) Kang, M.; Bhan, A. Kinetics and Mechanisms of Alcohol Dehydration Pathways on Alumina Materials. *Catal. Sci. Technol.* **2016**, *6*, 6667−6678.
(28) Prins, R. Location of the Spinel Vacancies in gamma-Al_2O_3. *Angew. Chem., Int. Ed.* **2019**, *58*, 15548−15552.
(29) Ashbrook, S. E.; Hodgkinson, P. Perspective: Current Advances in Solid-State NMR Spectroscopy. *J. Chem. Phys.* **2018**, *149*, No. 040901.
(30) Wang, Q.; Li, W.; Hung, I.; Mentink-Vigier, F.; Wang, X.; Qi, G.; Wang, X.; Gan, Z.; Xu, J.; Deng, F. Mapping the Oxygen Structure of gamma-Al_2O_3 by High-Field Solid-State NMR Spectroscopy. *Nat. Commun.* **2020**, *11*, No. 3620.
(31) Taoufik, M.; Szeto, K. C.; Merle, N.; Rosal, I. D.; Maron, L.; Trébosc, J.; Tricot, G.; Gauvin, R. M.; Delevoye, L. Heteronuclear NMR Spectroscopy as a Surface-Selective Technique: A Unique Look at the Hydroxyl Groups of γ-Alumina. *Chem. - Eur. J.* **2014**, *20*, 4038−4046.
(32) Chandran, C. V.; Kirschhock, C. E. A.; Radhakrishnan, S.; Taulelle, F.; Martens, J. A.; Breynaert, E. Alumina: Discriminative Analysis Using 3D Correlation of Solid-State NMR Parameters. *Chem. Soc. Rev.* **2019**, *48*, 134−156.
(33) Duong, N. T.; Nishiyama, Y. Satellite and Central Transitions Selective $^1H/\{^{27}Al\}$ D-HMQC Experiments at Very Fast MAS for Quadrupolar Couplings Determination. *Solid State Nucl. Magn. Reson.* **2017**, *84*, 83−88.
(34) Shi, L.; Deng, G. M.; Li, W. C.; Miao, S.; Wang, Q. N.; Zhang, W. P.; Lu, A. H. Al_2O_3 Nanosheets Rich in Pentacoordinate Al^{3+} Ions Stabilize Pt-Sn Clusters for Propane Dehydrogenation. *Angew. Chem., Int. Ed.* **2015**, *54*, 13994−13998.
(35) Saalwächter, K.; Graf, R.; Spiess, H. W. Recoupled Polarization-Transfer Methods for Solid-State $^1H-^{13}C$ Heteronuclear Correlation in the Limit of Fast MAS. *J. Magn. Reson.* **2001**, *148*, 398−418.
(36) Lesage, A.; Bardet, M.; Emsley, L. Through-Bond Carbon−Carbon Connectivities in Disordered Solids by NMR. *J. Am. Chem. Soc.* **1999**, *121*, 10987−10993.
(37) Goldbourt, A.; Vega, S.; Gullion, T.; Vega, A. J. Interatomic Distance Measurement in Solid-State NMR Between a Spin-1/2 and a Spin-5/2 Using a Universal REAPDOR Curve. *J. Am. Chem. Soc.* **2003**, *125*, 11194−11195.
(38) Wang, W.; Jiao, J.; Jiang, Y.; Ray, S. S.; Hunger, M. Formation and Decomposition of Surface Ethoxy Species on Acidic Zeolite Y. *Chemphyschem* **2005**, *6*, 1467−1469.
(39) Wang, W.; Hunger, M. Reactivity of Surface Alkoxy Species on Acidic Zeolite Catalysts. *Acc. Chem. Res.* **2008**, *41*, 895−904.
(40) Wang, Z.; Jiang, Y.; Baiker, A.; Huang, J. Pentacoordinated Aluminum Species: New Frontier for Tailoring Acidity-Enhanced Silica−Alumina Catalysts. *Acc. Chem. Res.* **2020**, *53*, 2648−2658.
(41) Zheng, A.; Liu, S.-B.; Deng, F. ^{31}P NMR Chemical Shifts of Phosphorus Probes as Reliable and Practical Acidity Scales for Solid and Liquid Catalysts. *Chem. Rev.* **2017**, *117*, 12475−12531.
(42) Kostestkyy, P.; Yu, J.; Gorte, R. J.; Mpourmpakis, G. Structure−Activity Relationships on Metal-Oxides: Alcohol Dehydration. *Catal. Sci. Technol.* **2014**, *4*, 3861−3869.
(43) Zhao, Z.; Xiao, D.; Chen, K.; Wang, R.; Liang, L.; Liu, Z.; Hung, I.; Gan, Z.; Hou, G. Nature of Five-coordinate Al in γ-Al_2O_3 Revealed by Ultra-High Field Solid-State NMR *ACS Cent. Sci.*, in press DOI: 10.1021/acscentsci.1c01497.